SWEDISH DEFENCE
RESEARCH AGENCY

FOI-R--0417--SE
February 2002
ISSN 1650-1942
Scientific report

Rahman Aljasmi

FMCW-radar

Signal Processing and Parameter Estimation

Sensor Technology
SE-581 11 Linköping

SWEDISH DEFENCE RESEARCH AGENCY, FOI
Sensor Technology
P.O. Box 1165
SE-581 11 Linköping
Sweden

FOI-R--0417--SE
Ferуary 2002
ISSN 1650-1942
Scientific report

Rahman Aljasmi

FMCW-radar

Signal Processing and Parameter Estimation

<table>
<tr><td rowspan="5">Issuing organization
Swedish Defence Research Agency, FOI
Sensor Technology
P.O. Box 1165
SE-581 11 Linköping
Sweden</td><td>Report number, ISRN
FOI-R--0417--SE</td><td>Report type
Scientific report</td></tr>
<tr><td colspan="2">Research area code
5. Combat</td></tr>
<tr><td>Month year
February 2002</td><td>Project no.
E2026</td></tr>
<tr><td colspan="2">Customers code
5. Commissioned Research</td></tr>
<tr><td colspan="2">Sub area code
51 Weapons and Protection</td></tr>
<tr><td rowspan="4">Author/s (editor/s)
Rahman Aljasmi</td><td colspan="2">Project manager
John Ottosson</td></tr>
<tr><td colspan="2">Approved by
Johan Söderström</td></tr>
<tr><td colspan="2">Sponsoring agency
FM</td></tr>
<tr><td colspan="2">Scientifically and technically responsible
Rahman Aljasmi</td></tr>
<tr><td colspan="3">Report title

FMCW-radar. Signal processing and Parameter Estimation</td></tr>
<tr><td colspan="3">Abstract

This report concerns the development of a real time algorithm to estimate the path parameters of a threat target, for protection of military hardware.
The target is assumed to move in a straight line with parameters pass distance, pass time and target velocity. To estimate the path parameters a number of measured ranges and range speeds are needed, which are obtained from one sensor in this study. The goal is to develop a method having high accuracy.
The received FMCW-signal, which is delayed by the transit time, is mixed with the transmitted FMCW-signal and analysed in two dimensions for further information.
The mixed (filtered) signal consists of two different frequencies i.e. the power is divided between these, which has negative effect on the estimation of range and radial velocity. To avoid this problem and to increase the signal power, one part of the frequency spectrum is shifted, the discontinuity is fixed and the estimate of range and velocity relative to the radar is refined by the periodogram method.
The parameters are solved by the Mean Least Square method in two steps and the result is a feasible value for the further search.
To optimise the path parameters, Maximum Likelihood method is studied and the minimum variance has been analysed with the Cramér Rao Lower Bound.</td></tr>
<tr><td colspan="3">Keywords
FMCW-radar, range, range speed, path parameters, Cramér Rao Lower Bound, signal processing.</td></tr>
<tr><td>Further bibliographic information</td><td colspan="2">Language English</td></tr>
<tr><td>ISSN 1650-1942</td><td colspan="2">Pages: 26</td></tr>
<tr><td></td><td colspan="2">Price acc. to pricelist</td></tr>
</table>

Utgivare
Totalförsvarets Forskningsinstitut, FOI

Sensor Technology
P.O. Box 1165
SE-581 11 Linköping
Sweden

Rapportnummer, ISRN
FOI-R--0417--SE

Klassificering
Vetenskaplig rapport

Forskningsområde
5. Bekämpning

Månad, år
Februari 2002

Projektnummer
E2026

Verksamhetsgren
5. Uppdragsfinansierad verksamhet

Delområde
51 VVS med styrda vapen

Författare/redaktör
Rahman Aljasmi

Projektledare
John Ottosson

Godkänd av
John Söderström

Uppdragsgivare/kundbeteckning
FM

Tekniskt och/eller vetenskapligt ansvarig
Rahman Aljasmi

Rapportens titel (i översättning)
FMCW-radar. Signalbehandling och parameteruppskattning

Sammanfattning

Rapporten behandlar utformningen av en realtids algoritm för estimering av ett hots banparametrar för att skydda militär hårdvara.
Hotet antas gå i en rätlinjig bana med parametrarna passageavstånd, passagetid och hastighet. För att estimera banparametrarna behövs ett antal mätdata för avstånd och radialhastighet vilket i denna studie erhålles med en enda sensor. Målet är att utveckla en metod med hög noggrannhet.
Den mottagna FMCW-signalen som är fördröjd på grund av sin löptid, blandas med den sända signalen. Den nedblandade signalen analyseras 2-dimensionellt för vidare information.
Den filtrerade (blandade) signalen består av två frekvenser mellan vilka effekten delas i två olika delar vilket påverkar interpolationen negativt. För att undvika detta problem och höja signaleffekten, skiftas den ena frekvensdelen till den andra och diskontinuiteten elimineras.
Banparametrarna löses sedan i två steg med Minsta Kvadrat-metoden. De bestämda värdena används som startvärden för den vidare optimeringen.
För optimeringen av banparametrarna studeras Maximum Likelihood-metoden och minsta variansen för parametrarna undersöks med Cramér Rao’s undre gräns.

Nyckelord

FMCW-radar, avstånd, radial hastighet, banparameter, Cramér Rao undre gräns, signalbehandling.

Övriga bibliografiska uppgifter

Språk Engelska

ISSN 1650-1942

Antal sidor: 26

Distribution enligt missiv

Pris: Enligt prislista

Contents

1. Introduction

This report presents the results of a theoretical study of the radar system for active protection. The concept of ”active protection ” was introduced in relatively recent time, and is currently in Russian use for the protection of various armour vehicles of military hardware.

An active protection system for the tank can be visualised as a closest-range anti-missile defence system that creates an active protection area at a safe distance around the vehicle. It is extremely important for a tank crew to be exactly and continuously aware of all the actual or potential threats present on the battlefield, so that the active protection system automatically takes care of those threats that are directly engaging the vehicle.

The aim of this study is to develop a radar system with the above-mentioned characteristics of threat interception at required distance, with high accuracy and high probability, making threat identification possible resulting in improved situational awareness and control capacity.

The uses of FMCW-radar and its opportunity to measure range and range speed have been exploited in the application. It is assumed that the target is moving along a linear path with constant velocity. This radar transmits a continuous wave that is reflected back to the receiver after hitting the target. The received signal, which is delayed by its transit time and changed in carrier frequency because of the doppler frequency shift, carries the information about the target's range and its range speed.

The received signal is mixed with the transmitted signal and analysed in two dimensions using the Fourier transform to measure the range and radial velocity. The refined range and range speed will be collected to estimate the target's path parameters.

The estimator that is used to estimate the path parameters is the Log-Maximum-likelihood function, which will be solved for maximum probability and compared with the Cramér Rao Lower Bound of the estimate.

The theoretical study of the Cramér Rao Lower Bound shows that the estimator is not unbiased when the pass range is close to zero. To gather information about the standard deviation in this region we made a study by estimating the pass range $\hat{R}_0$ 200 times for every given R_0.

Numerical control is done by comparing the error of estimated path parameters with the theoretically estimated standard deviation of the parameters.

2. Ballistic path and its geometry

We assume that we have a fixed sensor that can observe the range and the range speed of a target and then we assume that the target has constant speed and course. Now, we can describe the path of a target relative to the sensor by three parameters. We choose the parameters as the pass range to the sensor, R_0, the time of passing at this range, t_0, and the velocity of the target, ν as indicated in Fig. 2.1.
This choice of parameters gives the following expression for range and range speed of a target as a function of time

$$R = \sqrt{R_0^2 + \upsilon^2 (t - t_0)^2} \tag{2.1}$$

$$\frac{dR}{dt} = \dot{R} = \frac{\upsilon^2 (t - t_0)}{R} \tag{2.2}$$

For active protection the estimation of these three parameters must be done accurately, which in turn depends on the accuracy of measuring the range and the range speed of the target.

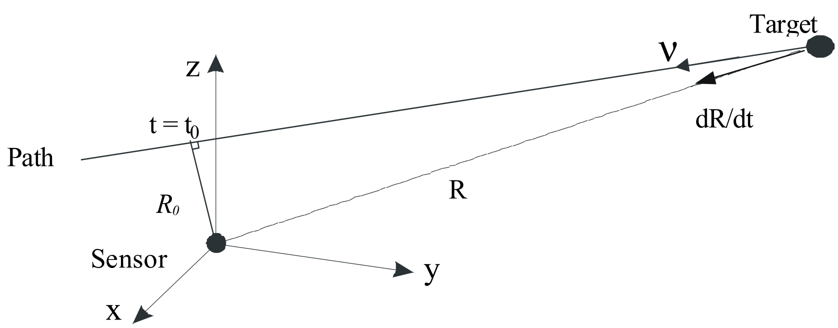

Fig. 2.1. The geometry of a target path relative to the sensor.

3. Radar system and waveform

FMCW-radar with a common antenna for the transmitted and received signals is studied in this report. The advantage of a CW-signal is that the signal can have low peak power. Fig. 3.1 illustrates such a radar.

A CW-system can lead to problems by way of transmitter leakage directly to the receiver, which can cause a fictitious stationary target ($\nu = 0$) at very short distance (≈ 0). The leak signal can also disturb the receiver's normal function if it is bigger than the receiver's dynamic range. Using a common antenna increases this problem. In many applications at very short ranges (e.g. < 500 m), it is possible to handle these problems. In this study we do not deal with these aspects, as we assumed that no signal leakage occurs and the study is limited to how the received signal depends on the range and range speed of the target.

3.1. Basic principles

Note in Fig. 3.2 that the bandwidth B and modulation period time T_m form a triangle similar to that formed by the beat frequency f_b and the transit time (delay time) τ. The relation between the bandwidth, modulation time, beat frequency and transit time is called the FMCW equation [1]

$$\frac{f_b}{\tau} = \frac{B}{T_m} \tag{3.1}$$

where $\tau = 2R/c$, R is the target range and c is the propagation velocity.

The range and the range speed resolution [2-3] are obtained by the equations (3.2) and (3.3).

$$\Delta R = \frac{c}{2B} \tag{3.2}$$

$$\Delta \dot{R} = \frac{\lambda}{2T_{obs}} = \frac{c}{2T_{obs} f_c} \tag{3.3}$$

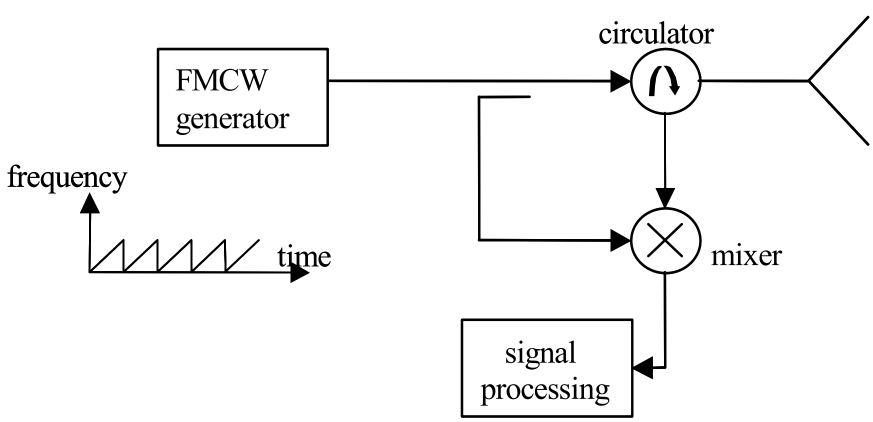

Fig. 3.1. Block diagram of FMCW radar.

where λ is the wave length, T_{obs} is the observation time and f_c is the carrier frequency. For the coherent signal, the movement of a target is limited to less than the range resolution ΔR, which makes the observation time T_{obs} to obey

$$T_{obs} < \frac{\Delta R}{\dot{R}_{max}} \tag{3.4}$$

where $\dot{R}_{max}$ is the maximum range speed of the target, of interest.
Equations (3.3) and (3.4) give the following condition for the product between the range and the velocity resolution.

$$\Delta R \cdot \Delta \dot{R} > \frac{c}{2f_c} \dot{R}_{max} \quad \text{or} \quad \frac{\Delta R \cdot \Delta \dot{R}}{\lambda \ \dot{R}_{max}} > \frac{1}{2} \tag{3.5}$$

The condition is fulfilled by the correct choice of waveform parameters.

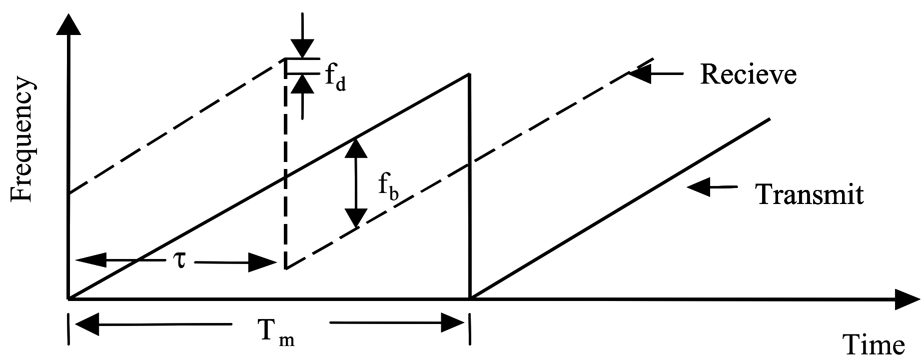

Fig. 3.2. Transmitted and received frequencies as a function of time showing beat frequency f_b and the doppler frequency f_d

4. Digital Signal Processing

The received signal is mixed, low-pass filtered and sampled according to Nyquist's sampling theorem. The filtered signal during one observation time is arranged in two dimensions where one dimension corresponds to the sample number within the modulation time and the other corresponds to the frequency sweep number within the observation time. The mixed signal consists of two different frequencies that produce two power spectral density peaks in the transform plane. By interpreting the transform plane dimensions as range and range speed the positions of the peaks give rough information about the range of a target and its closing speed. This information is refined to increase the accuracy of the measurements.

4.1. Wave model

The theory of FMCW and its waveform is found in [2-3]. In this job we study the linear sawtooth-FMCW waveform [1] with a modulation time less than 1 μs, an observation time less than 0.5 ms, a bandwidth between 10-500 MHz and 60 GHz carrier frequency.
The transmitted FMCW-signal in the complex plane can be defined as follows [4]

$$S_t(t) = \sqrt{P_t}A(t_n)e^{(j2\pi\phi(t_n))} \tag{4.1}$$

where

$$\begin{aligned} \phi(t) &= \int_{t_n} f(t)dt = (f_c - \frac{B}{2})t_n + \frac{B}{2T_m}t_n^2 + \phi_0 \\ t_n &= t - nT_m, \quad 0 \le t_n < T_m, \quad n = 0, 1, 2, \cdots, N-1. \end{aligned} \tag{4.2}$$

P_t is transmitted power, f_c is carrier frequency, B is bandwidth, T_m is modulation time and N is the number of periods. The number of periods is limited by the observation time T_{obs} ($T_{obs} >> T_m$) which is limited by the equations (3.4) and (3.5) for the unambiguous measurement. $A(t_n)$ is the normalized envelope of the signal and ϕ_0 is a constant phase equal to zero assuming that the signal is equal to zero when $t_n = 0$.
The received FMCW-signal is delayed by the transit time $\tau = 2R/c$, where R is the range and c is the velocity of propagation. The received signal can be expressed as follows

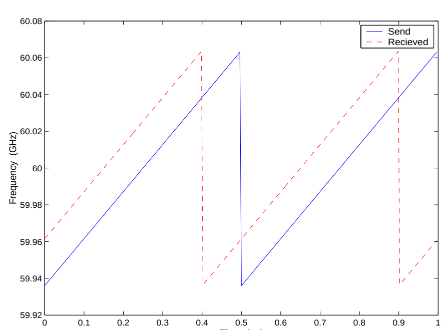

Fig. 4.1. Sent and received frequencies

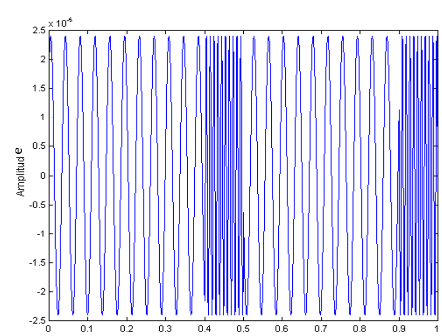

Fig. 4.2. Low frequency signal (the mixed signal)

$$S_r = \sqrt{P_r}\, A(t_n - \tau) e^{(j2\pi\phi(t_n - \tau))} + \omega(t) \tag{4.3}$$

where P_r [2-3] is the received power and $\omega(t) \in N(1,0)$ is complex white additive noise. The received signal is mixed with the transmitted signal, fed through a low-pass filter and sampled according to the Nyquist theorem. The result is a low-pass filtered signal in the base band, which has two frequencies in each period. Fig. 4.1 and Fig. 4.2 show a noise free signal reflected from a target at a range of 60 m.

4.2. 2-dimensional frequency spectrum

The low-pass filtered signal from a moving target (during an observation time) depends on three frequencies, the beat frequency (f_b), doppler frequency (f_d) that is included in the beat frequency, and B-f_b (B is bandwidth). The mixed signal and its phase function can approximately be defined as

$$S_{mix} \approx A \cdot e^{(j2\pi(\frac{2f_c \dot{R}}{c} nT_m + \frac{B}{T_m}\frac{2R}{c} t_n))} \tag{4.4}$$

where A is amplification and n is the number of periods or sweeps. We notice from equation (4.4) that the information about the range and range speed of a target is achieved by analysis of the signal in two dimensions. Therefore we arrange each period of the filtered data separately as a row or column of a matrix.
The first dimension consists of the number of periods and the second dimension of the sample number in each period. The 2-dimensional Fourier transform of this data gives the coarse information of range and range speed.
The standard deviation of radar [5] measurement is

$$\sigma = \pm \frac{M}{\sqrt{2 \cdot SNR}} \tag{4.5}$$

where M is the nominal resolution, where $M = \Delta R$ for the range and $M = \Delta \dot{R}$ for the range speed.
In order to accurately estimate the position and range speed of a target, we have tried the following methods: 2-dimensional interpolation [6], monopulse-method [7], zero padding and averaged periodogram-method [8]. The first two methods where attempted and did not generate satisfactory result. The zero padding and periodogram methods are mathematically the same, but because of the quantity of the data, the periodogram-method is more manageable.
The periodogram spectral estimator is

$$P_{per}(f_1, f_2) = \frac{1}{MN}\left|\sum_{m=0}^{M-1}\sum_{n=0}^{N-1} x[m, n] e^{-j2\pi(f_1 m + f_2 n)}\right|^2 \tag{4.6}$$

We search the frequency f_1 and f_2 that maximises the power spectral density.

5. Frequency estimation

The filtered signal consists of two different frequencies (a low and a high frequency) see Fig. 4.2. Depending on the signal frequencies and observation length, there are two different peaks in the frequency plane with different Power Spectral Density (PSD). Both peaks reflect the same waveform and target information.
The traditional method is to use the longest sequence. Short ranges to targets of interest often facilitate this where the travel time of the signal is short compared to the modulation time (T_m).
We are interested in signal travel times comparable to the modulation time and therefore we have studied the possibility of using the whole received data sequence to enhance the signal processing.
The frequency of one part of the sequence is shifted into the other one and the discontinuity between these two parts of the sequence is adjusted (see Fig. 5.1 and Fig. 5.2). Thereby we get a one-frequency signal with improved Power Spectral Density.

5.1. Frequency shifting

The filtered signals consist of two frequencies that result in two different peaks. To concentrate the power density to one position, we need to transform one frequency to the other using the Fourier transform theorem [6]

$$e^{j\omega_0 n} x[n] \quad \overset{\mathcal{F}}{\leftrightarrow} \quad X(\omega - \omega_0) \tag{5.1}$$

In order to shift one part of the sequence we have to find the breakpoint between the two parts (see Fig. 5.1) related to the target of interest. By inspection of the second derivative of the phase of the band-pass filtered signal we can get information about the position where the frequency shift occurs.
When we have found at which sample the shift occurs, we separate the time data from each other and shift the frequency of the shorter part to that of the longer part using (5.1).

$$x_s[n] = e^{j\omega_0 n} x_1[n] \tag{5.2}$$

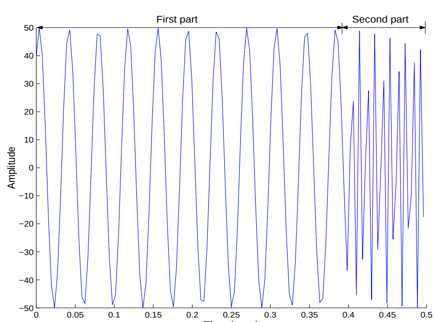

Fig. 5.1. Real part of time data showing two different frequencies.

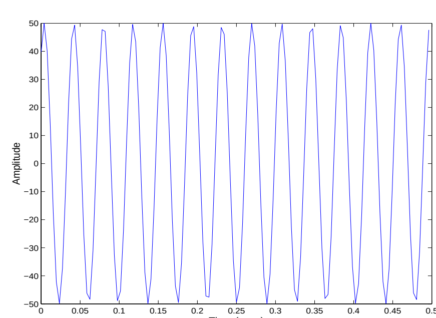

Fig. 5.2. Real part of time data shifted frequency and adjusted discontinuity.

where $x_1[n]$ is the shortest part of the time signal and ω_0 can be specified as radians/sample. In this case ω_0 is $\pi/2$ because the distance between these two peaks (see Fig. 5.3) in the frequency plane is always a quarter of a period.
A discontinuity in phase occurs at the breakpoint, which affects the spectral data.
To adjust the discontinuity between these two parts of the signals, we have to estimate the phase discrepancy between the x_s (the shifted frequency part of the signal) and the other part. The estimated phase deviation δ will be added to the phase of $x_s[n]$ as follows

$$x_{sf}[n] = e^{j\delta} x_s[n] \tag{5.3}$$

The x_{sf} will be put together with the first sequence. This procedure is applied to every period of the filtered signal. We show an example of the achieved result for a single target without noise in Fig. 5.4.
In a real situation with noise, it is not sufficient to use the procedure for every period of the signal. In this case we take the 2-dimensional FFT of the time signal and then the data row through the peaks in the frequency plane (along the range dimension, see Fig. 5.3) and apply an inverse FFT to that row.
The new signal is an average signal of the whole period that has been filtered and because of the higher SNR in this new signal, we can deal with it without having difficulty to find the boundary sample and adjust it to one frequency by the procedure explained above (see Fig. 5.1 and Fig. 5.2.).
There are two peaks that indicate the velocity of a target, see Fig. 5.3. These two peaks both correspond to the range speed of the target along the velocity direction and they are located at a certain distance from each other along the range direction.
We extract these two columns (along the velocity direction) from the left and right half plane (see Fig. 5.3) and apply the FFT inverse getting the time signals. These two signals will have the same frequency but with different phases (see Fig. 5.5). We estimate the phase difference and adjust one of the data series. We show an example in Fig. 5.6.

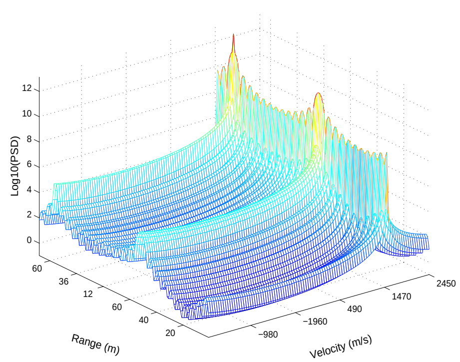

Fig. 5.3. 10-Logarithm of the Power Spectral Density when a target is moving with 2000 m/s at 60 m range, before frequency shifting (noise free signal).

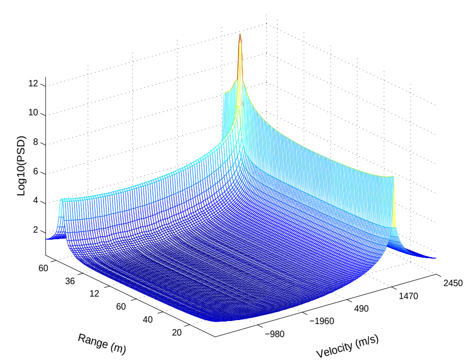

Fig. 5.4. 10- Logarithm of the Power Spectral Density when a target is moving with 2000 m/s at 60 m range, after frequency shifting (noise free signal).

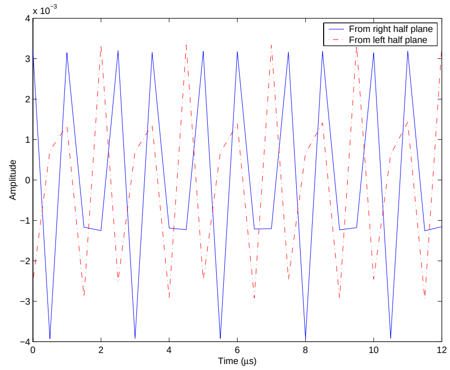

Fig. 5.5. Truncated time signals from left and right half planes in Fig. 5.3.

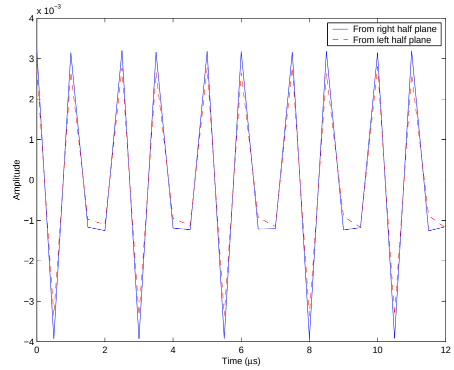

Fig. 5.6. Truncated time signal from left and right half planes with phase difference adjusted.

We add the data and get a new data series and an improved SNR.

6. Range and Range speed measurement

The transmitter frequency of FMCW radar is changed as a function of time in a known manner. If there is a reflecting object at a distance R, an echo signal will return after the round trip propagation time delay $\tau = 2R/c$. The dashed line in Fig. 6.1(a) represents the echo signal frequency. If there is no doppler frequency shift, the beat frequency (difference frequency) measured is due only to the range of the target.
In any practical CW radar, the frequency cannot be continuously changed in one direction only. Periodicity in modulation is necessary but the modulation is not necessarily being sawtooth as in the figure (it can be sinusoidal, triangular or some other shape). If the frequency is modulated at a rate $f_m = 1/T_m$ over a range B (bandwidth), the beat frequency is [1]

$$f_{b1} = B - f_{b2} \tag{6.1}$$

$$f_{b2} = \frac{2R}{c} B f_m \tag{6.2}$$

The measurement of the beat frequency determines the range R.
In the above discussion, the target was assumed to be stationary. If this assumption is not applicable, a doppler frequency shift will be superimposed on the FM range beat frequency and an erroneous range measurement results. The doppler frequency shift

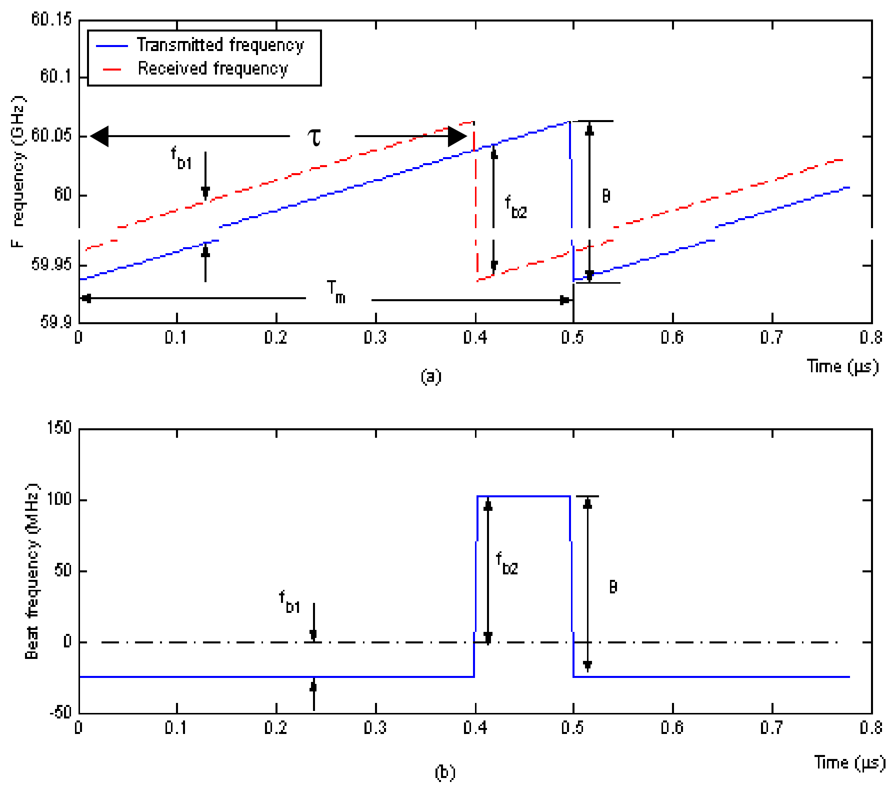

Fig. 6.1. Frequency-time relationship in FMCW-radar. (a) Sawtooth frequency modulation; (b) Beat frequency of (a).

causes the frequency of the echo signal to be shifted up or down and the beat frequency is

$$f_{b2} = \frac{2R}{c} B f_m + f_d \tag{6.3}$$

$$f_d = \frac{2f_c}{c} \dot{R} \tag{6.4}$$

where $\dot{R}$ is the target velocity relative to the radar and f_c is the carrier frequency.

7. Refinement of the frequency estimation

As we mentioned before, we use the periodogram-method to estimate the location of the power spectrum peak.
The sequence of the measured and sampled data from a target essentially depends on three frequencies, the doppler frequency shift, f_d, the beat frequency f_b, and B-f_b, where B is the bandwidth of the signal.
The doppler frequency shift (f_d), affects the beat frequency (f_b) when estimating range. We approximately adjust for this effect by solving a pair of equations (7.1) or (7.2).
If the position of the highest peak power density value is below the constant $B \cdot T_m$ (see Fig. 5.3), the equations to be solved are

$$\begin{cases} \frac{2B}{T_m c} R - \frac{2f_c}{c} \dot{R} = f_1 \\ -\frac{2f_c n}{c} \dot{R} = f_2 \end{cases} \tag{7.1}$$

Otherwise, if the position of the highest peak power density value is higher than $B \cdot T_m$, the equations will be

$$\begin{cases} B - \frac{2B}{T_m c} R - \frac{2f_c}{c} \dot{R} = f_1 \\ -\frac{2f_c n}{c} \dot{R} = f_2 \end{cases} \tag{7.2}$$

where B is bandwidth, T_m is modulation time, c is propagation velocity, f_c is carrier frequency, n is the number of periods or sweeps, f_1 and f_2 are the estimated frequencies for the range and range speed by the periodogram-method.

8. Numerical error analysis

For the analysis of the numerical errors of the procedure, we use noise free signals, to examine the accuracy of the measured range and radial velocity. Tab. 8.1 shows the three cases of constant target velocity, at different distances, with the target moving towards a sensor along a linear path i.e. the pass range of the target is zero ($R_0 = 0$), (see Fig. 2.1).

	Case 1	Case 2	Case 3
Velocity (m/s)	2241.79	1513.7	301.41
Range (m)	60, 50, 40, 30, 20, 10	60, 50, 40, 30, 20, 10	60, 50, 40, 30, 20, 10

Tab. 8.1

The parameters of the FMCW-signal are given in Tab. 8.2.

Notation	Parameters	Value
f_c	Carrier frequency	60 GHz
B	Bandwidth	128 MHz
T_m	Modulation time	0.5 μs
N	Number of period	100

Tab. 8.2

We estimate the range and radial velocity by estimating the position of the target power spectrum peak and calculate the corresponding range and radial speed where the associated measuring time is an average of the observation time. Fig. 8.1 and Fig. 8.2, show the results of the error calculation for the range and the radial velocity.

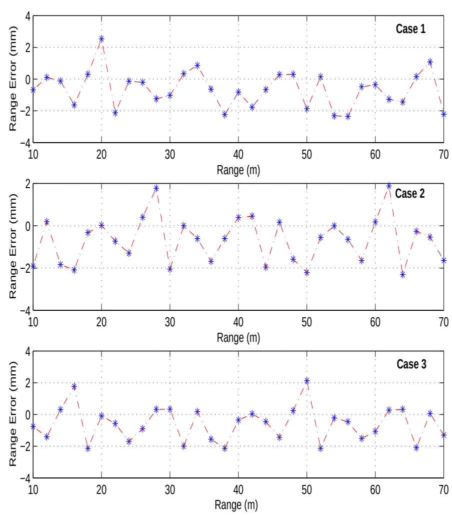

Fig. 8.1. Numerical error of measuring range.

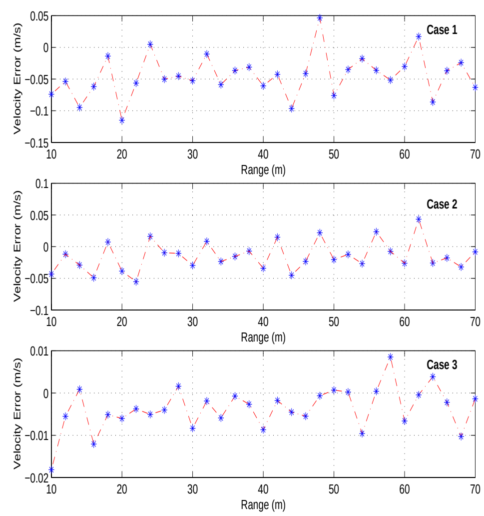

Fig. 8.2. Numerical error of measuring velocity.

9. Comparison of the measurements

The mixed FMCW signal consists of two different frequencies, see Fig. 5.1. The length of the different parts of the signal depends on the position of the target.
The traditional method of FMCW is that the longest part of the signal frequency will be analysed, while the shortest length will be filtered out. The disadvantage of this method is, that the signal power could be wasted up to 50%.
The proposed method has higher SNR but introduces some frequency error when shifting the frequency and adjusting the discontinuity. The introduced error makes the standard deviation of the measurements increase reasonably.
To compare these two methods we chose two different distances, 40 m and 60 m for a target with a range speed of 2000 m/s moving toward a sensor. We simulate 300 range and range speed measurements in each point; the result is presented below.

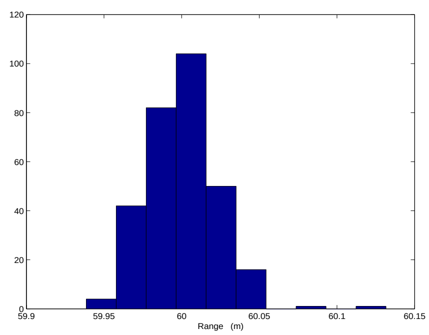

Fig. 9.1 The target position is measured 300 times at 60 m distance. The traditional method gives STD= 0.023 m.

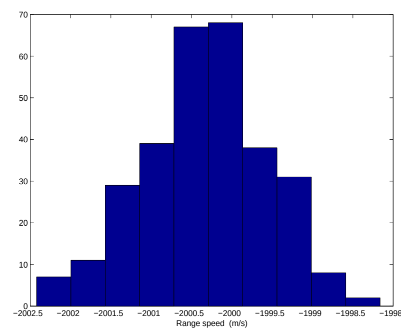

Fig. 9.2 The target range speed is measured 300 times at 60 m distance. The traditional method gives STD=0.843 m/s.

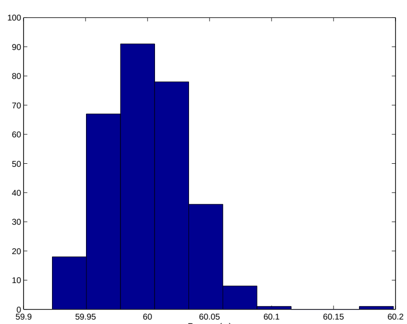

Fig. 9.3 The target position is measured 300 times at 60 m distance. The proposed method gives STD= 0.034 m.

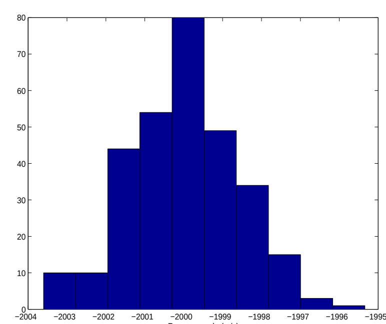

Fig. 9.4 The target range speed is measured 300 times at 60 m distance. The proposed method gives STD=1.391 m/s.

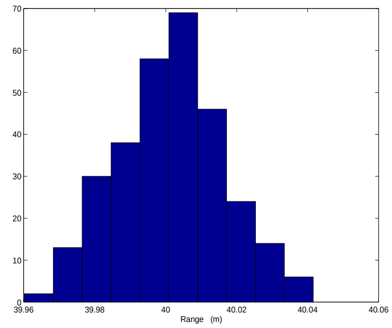

Fig. 9.5 The target position is measured 300 times at 40 m distance. The traditional method gives STD= 0.015 m.

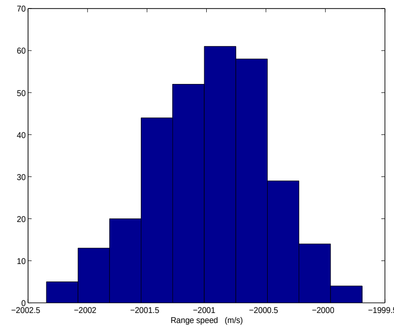

Fig. 9.6 The target range speed is measured 300 times at 40 m distance. The traditional method gives STD=1.099 m/s.

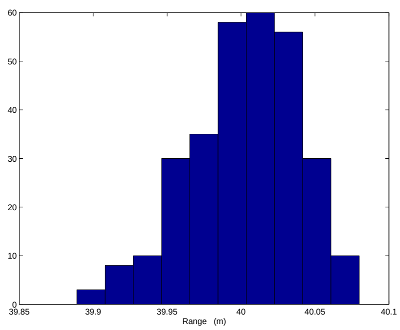

Fig. 9.7 The target position is measured 300 times at 40 m distance. The proposed method gives STD= 0.037 m.

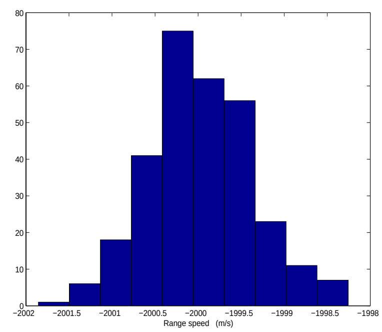

Fig. 9.8 The target range speed is measured 300 times at 40 m distance. The proposed method gives STD= 0.599 m/s.

If both parts of the signal are used, we can improve the SNR but at the same time we are increasing the error in the estimation of the range.

For the conventional method the standard deviation for range and range speed measurements at both distances are below 3 cm and 1.1 m/s respectively. The corresponding values of the proposed candidate method are 4 cm and 1.3 m/s.

We conclude that the proposed method is inferior to the conventional one and we therefore prefer the latter.

However, there still may be some more efficient method to use the full set of data.

10. Path parameter estimation

We use the least-square method in two steps to get the first estimation of the parameter $\overline{\boldsymbol{\theta}}$ = [R_0, ν, t_0]. We enhance these estimates using the maximum-likelihood method and assume that the measured range and range speed data are uncorrelated.
Then we search the values corresponding to the maximum probability using the first estimates as starting values.

10.1. Least-square method

The range and radial velocity of a target in an observation time can be expressed as

$$R[t_n, \overline{\boldsymbol{\theta}}] = \sqrt{R_0^2 + \boldsymbol{\nu}^2 [t_n - t_0]^2} \tag{10.1}$$

$$\dot{R}[t_n, \overline{\boldsymbol{\theta}}] = \frac{\boldsymbol{\nu}^2 [t_n - t_0]}{R[t_n, \overline{\boldsymbol{\theta}}]} \tag{10.2}$$

where t_n is the mean time of the n:th observation time interval and n = [1, 2, .., N] there N is the number of observations used for the path parameter estimation. The quantity $\overline{\boldsymbol{\theta}}$ = [R_0, ν, t_0].
We are going to solve the path parameters [R_0, ν, t_0] using a least-square method. In one case we first eliminate the parameter R_0 by multiplying equation (10.1) with equation (10.2) as follows

$$R[t_n, \overline{\boldsymbol{\theta}}] \cdot \dot{R}[t_n, \overline{\boldsymbol{\theta}}] = \boldsymbol{\nu}^2 [t_n - t_0] \tag{10.3}$$

We then estimate the two parameters (ν, t_0) by the least-square method and then we estimate R_0 from equation (10.1).

10.2. Maximum-likelihood method

We proceed with applying the optimal maximum-likelihood method. The method gives an asymptotic optimum when solving the parameters for maximum probability.
We assume that the measured data are normal-distributed with standard deviation [2] for measured range and range speed

$$\boldsymbol{\sigma}_{R_n} = \frac{\Delta R}{\sqrt{2 \cdot SNR_{init}}} \cdot \frac{\hat{R}_n^2}{R_{max}^2} \tag{10.4}$$

$$\boldsymbol{\sigma}_{\dot{R}n} = \frac{\Delta \dot{R}}{\sqrt{2 \cdot SNR_{init}}} \cdot \frac{\hat{R}_n^2}{R_{max}^2} \tag{10.5}$$

where ΔR and $\Delta \dot{R}$ is the resolution in range and range speed respectively, $\hat{R}_n$ is the measured range in observation number n and R_{max} denotes the maximum range.
We can now write the normal-distribution function for range and range speed as follows

$$P[R_n] = \frac{1}{\boldsymbol{\sigma}_{R_n}\sqrt{2\boldsymbol{\pi}}}\,\mathrm{Exp}\left(-\left(\frac{R_n - R[t_n, \overline{\boldsymbol{\theta}}]}{2\boldsymbol{\sigma}_{R_n}}\right)^2\right) \tag{10.6}$$

$$P[\dot{R}_n] = \frac{1}{\boldsymbol{\sigma}_{\dot{R}_n}\sqrt{2\boldsymbol{\pi}}}\,\mathrm{Exp}\left(-\left(\frac{\dot{R}_n - \dot{R}[t_n, \overline{\boldsymbol{\theta}}]}{2\boldsymbol{\sigma}_{\dot{R}_n}}\right)^2\right) \tag{10.7}$$

where R_n and $\dot{R}_n$ is the measured range and range speed for the current point n = [1, 2, 3, …, N].
Furthermore we assume that the measured data (range and range speed) are uncorrelated and we get the following expression for the maximum likelihood function.

$$L[\mathbf{R}, \dot{\mathbf{R}}, \overline{\theta}] = \prod_{n=1}^{N}\prod_{n=1}^{N} P[R_n]\cdot P[\dot{R}_n] =$$

$$\frac{1}{(2\pi)^N \prod_{n=1}^{N}\left(\sigma_{R_n}\,\sigma_{\dot{R}_n}\right)}\exp\left(-\frac{1}{2}\sum_{n=1}^{N}\left(\left(\frac{R_n - R[t_n, \overline{\theta}]}{\sigma_{R_n}}\right)^2 + \left(\frac{\dot{R}_n - \dot{R}[t_n, \overline{\theta}]}{\sigma_{\dot{R}_n}}\right)^2\right)\right) \tag{10.8}$$

where $\mathbf{R}$ and $\dot{\mathbf{R}}$ denotes the vector of the measured range and range speed with a length N, and $\theta = [\ R_0, \nu, t_0\ ]$ is the vector parameter .
Maximising the likelihood function, L, is equivalent to minimising the negative log-likelihood function, -S. The Log-likelihood function S is defined as

$$S[\mathbf{R}, \dot{\mathbf{R}}, \overline{\boldsymbol{\theta}}] = \ln(L) = C - \frac{1}{2}\sum_{n=1}^{N}\left(\left(\frac{R_n - R[t_n, \overline{\boldsymbol{\theta}}]}{\boldsymbol{\sigma}_{R_n}}\right)^2 + \left(\frac{\dot{R}_n - \dot{R}[t_n, \overline{\boldsymbol{\theta}}]}{\boldsymbol{\sigma}_{\dot{R}_n}}\right)^2\right) \tag{10.9}$$

where C is a constant.
By minimizing the negative log-likelihood function with respect to $\overline{\boldsymbol{\theta}}$, we obtain an estimate, $\hat{\overline{\boldsymbol{\theta}}}$, of the vector parameters.

11. Cramér-Rao analysis

The Cramér-Rao bound gives the minimum variance of the estimated parameters. We will analyse our estimate theoretically and compare with this theoretical limit. However, this limit is a bound on unbiased estimators, so if our algorithm results in an unbiased estimate or not, is relevant and has to be decided.
The knowledge of minimum variance is the important part, because it serves as a guideline for optimising the estimate and to understanding how it should be formulated.
The minimum variance of the unbiased estimator is defined as follows [9]

$$\operatorname{var}[\hat{\bar{\boldsymbol{\theta}}}_i] \;\geq\; \left[\mathrm{F}[\bar{\boldsymbol{\theta}}]^{-1}\right]_{ii} \tag{11.1}$$

where F is the Fisher information matrix, $\hat{\theta}$ is the estimate of the vector parameter $\theta = [\ R_0,\ \nu,\ t_0\ ]$ and i denotes the component in the estimate and the Fisher matrix, respectively. The element of the Fisher matrix is defined as

$$\left[\mathrm{F}[\bar{\boldsymbol{\theta}}]\right]_{ij} = -\mathrm{E}\left[\frac{\partial^2}{\partial\boldsymbol{\theta}_i\partial\boldsymbol{\theta}_j}\mathrm{S}[\mathrm{R},\dot{\mathrm{R}},\bar{\boldsymbol{\theta}}]\right] \tag{11.2}$$

where i and j denote the vector parameter component and at the same time the row and column respectively in Fisher's information matrix.
The first partial derivation of the log-likelihood function with respect to a component of vector parameters is

$$\begin{aligned}\frac{\partial}{\partial\boldsymbol{\theta}_i}\mathrm{S}[\mathrm{R},\dot{\mathrm{R}},\bar{\boldsymbol{\theta}}] &= \sum_{n=1}^{N}\frac{(\mathrm{R}_n-\mathrm{R}[t_n,\bar{\boldsymbol{\theta}}])}{\boldsymbol{\sigma}^2_{\mathrm{R}_n}}\frac{\partial}{\partial\boldsymbol{\theta}_i}\mathrm{R}[t_n,\bar{\boldsymbol{\theta}}]+\\ &+\sum_{n=1}^{n}\frac{(\dot{\mathrm{R}}_n-\dot{\mathrm{R}}[t_n,\bar{\boldsymbol{\theta}}])}{\boldsymbol{\sigma}^2_{\dot{\mathrm{R}}_n}}\frac{\partial}{\partial\boldsymbol{\theta}_i}\dot{\mathrm{R}}[t_n,\bar{\boldsymbol{\theta}}]\end{aligned} \tag{11.3}$$

The second partial derivative is

$$\begin{aligned}\frac{\partial^2}{\partial\boldsymbol{\theta}_i\partial\boldsymbol{\theta}_j}\mathrm{S}[\mathrm{R},\dot{\mathrm{R}},\bar{\boldsymbol{\theta}}] &= -\sum_{n=1}^{N}\frac{1}{\boldsymbol{\sigma}^2_{\mathrm{R}_n}}\frac{\partial}{\partial\boldsymbol{\theta}_i}\mathrm{R}[t_n,\bar{\boldsymbol{\theta}}]\frac{\partial}{\partial\boldsymbol{\theta}_j}\mathrm{R}[t_n,\bar{\boldsymbol{\theta}}]+\\ &+\sum_{n=1}^{N}\frac{(\mathrm{R}_n-\mathrm{R}[t_n,\bar{\boldsymbol{\theta}}])}{\boldsymbol{\sigma}^2_{\mathrm{R}_n}}\frac{\partial^2}{\partial\boldsymbol{\theta}_i\partial\boldsymbol{\theta}_j}\mathrm{R}[t_n,\bar{\boldsymbol{\theta}}]\\ &-\sum_{n=1}^{N}\frac{1}{\boldsymbol{\sigma}^2_{\dot{\mathrm{R}}_n}}\frac{\partial}{\partial\boldsymbol{\theta}_i}\dot{\mathrm{R}}[t_n,\bar{\boldsymbol{\theta}}]\frac{\partial}{\partial\boldsymbol{\theta}_j}\dot{\mathrm{R}}[t_n,\bar{\boldsymbol{\theta}}]+\\ &+\sum_{n=1}^{N}\frac{(\dot{\mathrm{R}}_n-\dot{\mathrm{R}}[t_n,\bar{\boldsymbol{\theta}}])}{\boldsymbol{\sigma}^2_{\dot{\mathrm{R}}_n}}\frac{\partial^2}{\partial\boldsymbol{\theta}_i\partial\boldsymbol{\theta}_j}\dot{\mathrm{R}}[t_n,\bar{\boldsymbol{\theta}}]\end{aligned} \tag{11.4}$$

Note that the stochastic variables are R_n and $\dot{R}_n$. The parameters $R[t_n, \bar{\boldsymbol{\theta}}]$ and $\dot{R}[t_n, \bar{\boldsymbol{\theta}}]$ are non-linear which makes the equation (11.4) a non-linear equation.

An unbiased estimator is denoted by $E[R_n] = R[t_n, \bar{\boldsymbol{\theta}}]$ and $E[\dot{R}_n] = \dot{R}[t_n, \bar{\boldsymbol{\theta}}]$. Then the Fisher information matrix takes the shorter form

$$\begin{aligned}\left[F[\bar{\boldsymbol{\theta}}]\right]_{ij} &= \sum_{n=1}^{N} \frac{1}{\boldsymbol{\sigma}_{R_n}^2} \frac{\partial}{\partial \boldsymbol{\theta}_i} R[t_n, \bar{\boldsymbol{\theta}}] \frac{\partial}{\partial \boldsymbol{\theta}_j} R[t_n, \bar{\boldsymbol{\theta}}] + \\ &+ \sum_{n=1}^{N} \frac{1}{\boldsymbol{\sigma}_{\dot{R}_n}^2} \frac{\partial}{\partial \boldsymbol{\theta}_i} \dot{R}[t_n, \bar{\boldsymbol{\theta}}] \frac{\partial}{\partial \boldsymbol{\theta}_j} \dot{R}[t_n, \bar{\boldsymbol{\theta}}]\end{aligned} \tag{11.5}$$

The results of the Cramér Rao Lower Bound for these three parameters are shown below. The CRLB is the minimum variance that we can achieve for an unbiased estimator.
The standard deviation of R_0 goes to infinity as R_0 goes to zero. The reason is that the Fisher information matrix becomes singular in this point and the information is no longer valid (the processor is no longer unbiased).

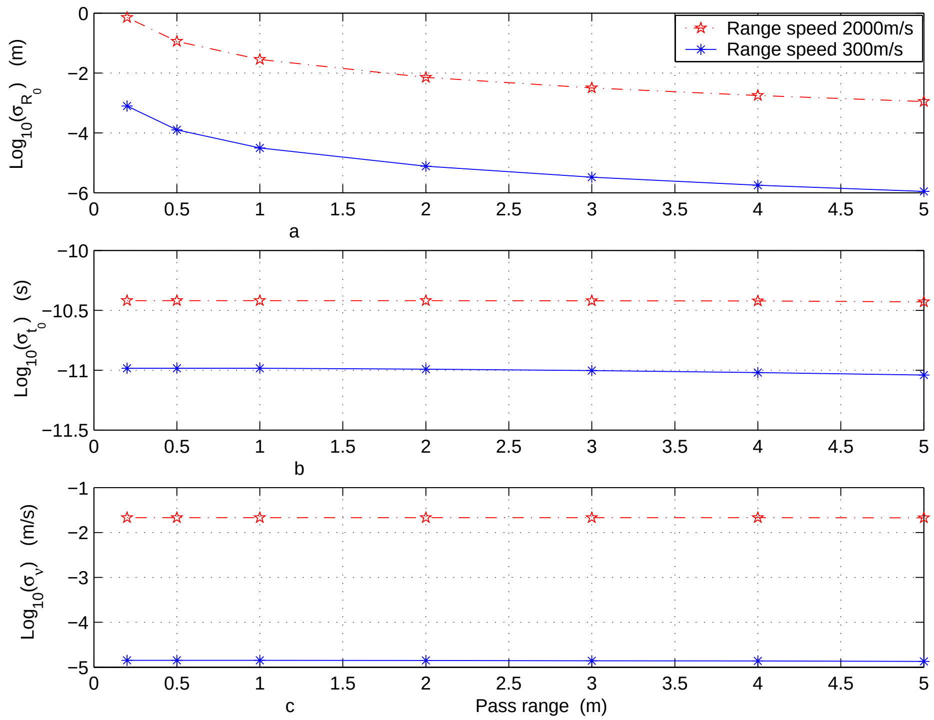

Fig. 11.1. The CRLB of the parameters R_0 (a), t_0 (b), ν (c).

12. Numerical error analysis

In order to analyse the performance of the path parameter estimation procedure, we compare the result with the Cramér-Rao Lower Bound, which gives the lowest variance when estimating the parameters for an unbiased process.

To estimate the path parameters [R_0, ν, t_0], we will solve the likelihood function for the maximum of probability (10.9) assuming that the process is unbiased. We have performed 200 estimations of $\hat{R}_0$ for every given R_0, and calculated the standard deviation. Fig. 12.1 shows the result compared with the Cramér Rao lower bound.

The range and the range speed are measured by the proposed method in this case and the pass range is estimated from the collected data of the measured range and range speed for the maximum of the probability. The standard deviation of the estimated pass range is rather high as indicated in section 9.

We have to find the optimal combination between the signal bandwidth, modulation time and the number of the signal periods to get a better estimation but this issue is not included in this report.

In Fig. 12.1 the Cramér Rao Lower bound goes to infinity as pass range goes to zero. The reason is that the Fisher information matrix (see equation (11.5)) becomes singular and the information is no longer valid. The processor is biased in this region.

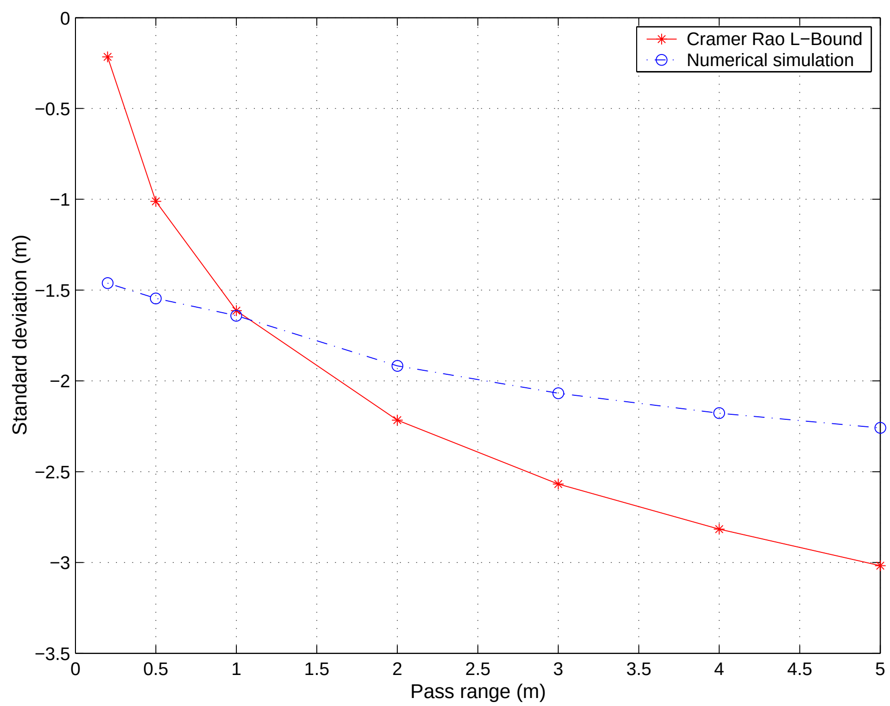

Fig. 12.1. Standard deviation of the pass range in comparison with Cramér Rao Lower Bound.

13. Conclusion

This work is mainly supported by simulations implemented in Matlab-programs. We have studied an FMCW-radar measuring a point target in free space. We have accounted for the thermal noise of the system but neglected e.g. target glint and multi-path phenomena occurring in real situations.

The mixed FMCW-signal during a frequency sweep consists of two parts at two different frequencies. Traditionally, only the longest part of the signal is used for signal processing but we have studied the possibility to merge the parts and thereby increase the SNR in the following signal processing.

A periodogram spectral estimator estimates the position of spectral peaks and from the location the corresponding range and range speed are calculated.

We have calculated the range and range speed from a number of simulations and compared with the input data. The error shows negligible bias and the maximum error is about 3 mm and 12 cm/s for range and range speed respectively, as indicated in Fig. 8.1 and Fig. 8.2.

For estimation of the path parameters (pass range (R_0), pass time (t_0) and path speed (v)), from a collected number of consecutive range and range speed data we use the minimum least square method, which is not optimal. The result is used as a start value for the further search for an optimum.

To validate the signal processing and estimation procedure we have studied the Cramér Rao Lower Bound (CRLB) with a number of simulations (200) for certain choices of path parameters (see Fig. 12.1). The result indicates that the estimate is biased in the region $0< R_0 <1.5$. Due to the biased estimation the CRLB is not valid within this interval. For $R_0>1.5$ we notice an increasing difference between the standard deviation of our estimation and the corresponding CRLB-limit. We suspect that the main reason for the difference is the nonlinear velocity variation within a single measurement interval. The measurement time interval is 0.5 ms corresponding to the range interval 1 m for the target speed 2000 m/s. The nonlinearity affects the solution of the range and range speed by equation (7.1) and (7.2). Another reason is the estimation of the phase difference between two parts of the signal, which can insert some error joining the signal parts together.

This study comprises only one sensor measuring range and range speed and therefore only a limited set of the path parameters can be determined. We need at least three sensors of this type for a complete parameter determination (the position vector at a known time and the velocity vector, 6 parameters).

Acknowledgements

The author’s tanks are due to Jan Kjellgren, for all support in the course of this work and to Ain Sume for reviewing the report.

References

[1] James A. Scheer, James L. Kurtz (editors). “Coherent Radar Performance Estimation”. Boston: Artech House (1993), ISBN 0-89006-628-0.

[2] Merill I. Skolnik. ”Introduction to Radar Systems”. Tokyo: McGraw-Hill, 2nd Edition (1980), ISBN 0-07-066572-9.

[3] Merill Skolnik. “Radar Handbook”. New York: McGraw-Hill Publishing Company (1990), ISBN 0-07-057913-X.

[4] David K. Barton. ”CW and Doppler Radar”, Radars Vol. 7 (ed. D.K. Barton). Dedham: Artech House, 1978, ISBN 0-89006-075-4.

[5] Ain Sume. “Kursmaterial i radarteori ”. Linköping: FOA-D--95-00108-3.3--SE, April 1995.

[6] Alan V. Oppenheim & Ronald W. Schafer.”Discrete-Time Signal Processing”. Englewood Cliffs: Prentice Hall (1989), ISBN 0-13-216771-9.

[7] Nadav Levanon. “Radar Principles”. New York: John Wiley & Sons (1988),

ISBN 0-471-85881-1.

[8] Steven M. Kay. “Modern Spectral Estimation: Theory & Application”. Englewood Cliffs : Prentice Hall (1988), ISBN 0-13-598582-X.

[9] Steven M. Kay. “Fundamentals of Statistical Signal Processing: Estimation Theory”. Prentice Hall International Editions (1993). ISBN 0-13-042268-1.